

Charge symmetry tested by comparison of π^+ and π^- elastic scattering from deuterium at 143 MeV

T. G. Masterson, J. J. Kraushaar, R. J. Peterson, R. S. Raymond, and R. A. Ristinen
Nuclear Physics Laboratory, Department of Physics, University of Colorado, Boulder, Colorado 80309

R. L. Boudrie

*Clinton P. Anderson Meson Physics Facility, Los Alamos National Laboratory,
 Los Alamos, New Mexico 87545*

E. F. Gibson

Physics Department, California State University, Sacramento, California 95819

A. W. Thomas*

TRIUMF, Vancouver, Canada V6T 2A3

(Received 1 July 1982)

A sensitive test of nuclear charge symmetry has been made by comparing differential cross sections for π^+ and π^- elastic scattering from deuterium at 143 MeV. Residual charge symmetry breaking effects in the cross section ratio have been parametrized in terms of mass and width differences among the components of the Δ isobar. Accurate absolute π^-d differential cross sections were measured for the first time and π^+d differential cross sections agree well with other results and with three-body calculations.

NUCLEAR REACTIONS ${}^2\text{H}(\pi^+, \pi^+)$, ${}^2\text{H}(\pi^-, \pi^-)$, $E_\pi = 143$ MeV, measured $\sigma(\theta)$. Magnetic spectrograph. Three-body analysis. Charge symmetry breaking parametrized in terms of Δ isobar mass and width differences.

I. INTRODUCTION

It is generally assumed that the strong interaction is charge symmetric, that is, identical under the inversion of the third component of the isospin operator. This leads, for instance, to the equality of the nn and pp nuclear interactions and to the mirror symmetry found in light nuclei.

The inversion of the T_3 component of the isospin of the π^+d system results in the π^-d system, and hence a comparison of π^+d and π^-d nuclear cross sections provides a sensitive and direct test of charge symmetry. Both total and differential nuclear cross sections for π^+ and π^- scattering from deuterium should be equal. In each case, however, corrections must be made for Coulomb effects to obtain the purely nuclear cross section since the electromagnetic interaction violates charge symmetry.

In this paper we present a detailed description of our π^+d and π^-d differential cross section mea-

surements, and of the accurate measurement of the ratio of the difference between these cross sections to the sum. Theoretical estimates of electromagnetic corrections to this ratio are then made and the extent to which charge symmetry is violated in this interaction is determined. A brief description of the differential cross section ratio data has already been published as a Letter by Masterson *et al.*¹

Pedroni *et al.*² have made measurements of $\pi^\pm d$ total cross sections from 70 to 370 MeV which indicated possible charge symmetry violations at the 3–8% level. These differences between π^+d and π^-d total cross sections persisted after Coulomb and Coulomb-nuclear interference corrections; these were parametrized in terms of mass and width differences among the components of the Δ_{33} isobar in a way similar to that indicated by Myhrer and Pilkuhn.³

In Sec. II the current status of experimental observations related to charge symmetry is reviewed and estimates of the sensitivity of elastic pion

scattering to charge symmetry breaking effects are presented. Three-body descriptions of the πd interaction obtained from exact solutions of Faddeev⁴ equations are also discussed there.

The π^+d and π^-d differential cross sections were measured at a pion energy of 143 MeV to match the energy at which the maximum asymmetry in the total cross sections was observed. It was also at this energy that $\pi^\pm p$ differential cross sections were measured by Bussey *et al.*⁵ and these were used as a basis for the absolute normalizations for the πd system. There have been no previous measurements of π^-d differential cross sections in this energy region except for the early bubble chamber measurements of Pewitt *et al.*⁶ The present π^+d differential cross sections agree very well with recent π^+d measurements of Gabathuler *et al.*⁷ and with the three-body calculations of Giraud *et al.*⁸ Our most precise result is the ratio of the difference of π^-d and π^+d differential cross sections to the sum

$$A_\pi = \frac{\sigma_{\pi^-}(\theta) - \sigma_{\pi^+}(\theta)}{\sigma_{\pi^-}(\theta) + \sigma_{\pi^+}(\theta)}. \quad (1.1)$$

The precision of this result is due to the cancellation of many absolute experimental and theoretical uncertainties in the ratio. Experimental details are discussed in Sec. III.

Electromagnetic corrections are required to make a comparison of π^+d and π^-d nuclear interactions and they are discussed in Sec. IV. These corrections arise from interference of Coulomb and nuclear amplitudes, and differences in effective π^+ and π^- interaction energies. Explicit charge asymmetric effects come from mass differences among the components of the Δ . The nuclear description of the πd system used to generate these corrections was the three-body Faddeev formalism of Rinat and Thomas.⁹⁻¹² The description was "fully" relativistic and included all S and P wave pion nucleon phase shifts. It is in the reliability of these corrections for the relatively well understood πd system that pion scattering from deuterium provides a more definitive test of charge symmetry than does pion scattering from heavier self-conjugate nuclei.

The charge symmetry violating effects that have been observed in this experiment can be expressed in terms of a Δ isobar mass difference parameter C_W with a value of 4.35 ± 0.5 MeV. This value is based on $\pi^\pm p$ normalization cross sections calculated from a standard set of $\pi^\pm p$ phase shifts. In the final section the implications of our results and com-

parisons with other tests of charge symmetry are discussed.

II. THEORETICAL AND EXPERIMENTAL BACKGROUND

The πd system has been studied intensively for the past several years and accurate calculations are now available for this simplest pion-nucleus system. The nonrelativistic three-body problem was first formulated by Faddeev⁴ in 1961 and then applied^{13,14} to the πd system in about 1972. The state of the art until then had consisted of single scattering plus some estimate of double scattering¹⁵ or a Glauber calculation.¹⁶ This was followed by attempts to understand the problems of double counting and absorption^{17,18} and exact solutions were obtained, both at zero energy¹⁸⁻²¹ and in the resonance region.^{13,22-24}

The pion is quite relativistic ($\beta > 0.85$) in this energy region and relativistic kinematics have been included in the πd descriptions of Rinat, Thomas, and others.⁹⁻¹² Initial three body relativistic calculations were without spin²⁵ and then later with all spin angular momentum complications.¹⁰⁻¹² More recent calculations by Giraud *et al.*,^{8,26} have included all S and P pion-nucleon partial waves and realistic deuteron wave functions as well as being fully relativistic. These calculations also include estimates of vector and tensor polarization observables. Recently it has been rigorously established that possible effects of pion absorption²⁷⁻³¹ can be exactly incorporated into a set of coupled integral equations in qualitative agreement with the original ansatz of Afnan and Thomas.³² For a more detailed review of each of these stages of development of the theory and its relevance to the more general question of pion-nucleus scattering, we refer to the recent review of Thomas and Landau.³³

These most recent calculations, both with^{27,34,35} and without²⁶ absorption, agree very well with elastic π^+d differential cross sections below the resonance. Calculations including absorption describe the minimum⁷ in the 256 MeV angular distribution better than those without, although calculated cross sections at back angles are still³³ higher than the data.

In the past couple of years both vector polarization³⁶ (iT_{11}) and tensor polarization^{37,38} (T_{20}) have been measured in πd scattering. The vector polarization at 142 MeV was fit rather well by a three-body calculation^{12,33,39} while the discrepancy at 256 MeV initially caused a great deal of dibaryonic exci-

tation.^{36,39,40} More recently it has been realized that very small changes⁴⁰ in the two or three dominant partial wave amplitudes can also explain the data. The discrepancies among T_{20} data sets^{37,38} and calculations³⁹ at 142 MeV are large. This is perhaps due to the manner in which absorption is treated^{27,35} and it may be some time before this is understood. None of these recent developments is included in this analysis.

All of the calculations discussed above have assumed nuclear charge symmetry which implies that the nuclear interaction is invariant under the inversion of the T_3 component of the isospin of every particle in the system. A review of the experimental and theoretical status of charge dependence in the nucleon-nucleon system through 1978 is given by Henley and Miller.⁴¹ The classical comparison of nn and pp interactions is plagued at low energy by a large Coulomb correction⁴² which changes the pp scattering length in a model dependent way from -7.82 ± 0.01 to -17.2 fm. (The estimated error of the corrected value is somewhat controversial, varying from 0.2 to many femtometers.⁴²) There has been no direct measurement for the nn system. Therefore the nn scattering length must be deduced either from nd scattering or from the $\pi^-d \rightarrow \gamma nn$ reaction and this results in large errors ($a_{nn} = -18.4 \pm 1.2$ fm). The nucleon-nucleon asymmetry parameter,

$$(a_{nn}^2 - a_{pp}^2)/(a_{nn}^2 + a_{pp}^2)$$

is equal to -0.05 ± 0.53 , where the error in a_{pp} is taken to be ± 3 fm as given by Henley and Miller.⁴¹ This may be compared with the integral of the pion differential asymmetry parameter A_π defined above.

Recently there have been calculations^{43,44} of the amount of charge symmetry breaking expected in the NN interaction due to quark mass differences and explicitly including the η' meson and magnetic couplings of the η mesons. Although cancellations give rise to large uncertainties, significant effects are predicted for the difference between nn and pp scattering lengths. The status of experiments and calculations now in progress on charge symmetry breaking in the $n-p$ system is discussed in the proceedings⁴⁵ of a Charge Symmetry Breaking Workshop held in Vancouver in 1981.

Another test of the validity of charge symmetry is provided by the difference in the binding energies of mirror nuclei. The simplest and most investigated pair is ${}^3\text{H}$ and ${}^3\text{He}$. After correction for Coulomb effects any difference in binding energy should be due to charge asymmetry between nn and

pp forces. (This neglects three-body forces.) It is worth noting that even rather sophisticated three-body Faddeev^{46,47} calculations are in disagreement with the binding energy of both ${}^3\text{H}$ and ${}^3\text{He}$ by about 1.2 and 0.1 MeV, respectively, and indicate a possible 1–15% asymmetry between nn and pp forces, strongly dependent on the NN potential used. The difference in binding energies is less model dependent. The ${}^3\text{H}$ binding energy⁴⁷ is 8.482 MeV while that of ${}^3\text{He}$ is 7.718 MeV. The difference in binding energies is 0.764 MeV as compared with 0.68 MeV expected from Coulomb corrections.⁴⁸ This asymmetry is further supported by Grüber's recent review⁴⁹ of low energy charged particle reaction and polarization data for the three body system.

In the intermediate energy πd system, most of the above problems are smaller. The inversion of the T_3 component of the isospin of the π^+d system gives the π^-d system and both are experimentally available. The Coulomb corrections are much smaller at intermediate energies.

Recently Hollas *et al.*⁵⁰ reported a measurement of charge symmetry breaking by determining the asymmetry of the angular distribution about 90° in the center of mass scattering angle for the deuteron in the $np \rightarrow d\pi^0$ reaction at an energy of 795 MeV. They found no evidence for an asymmetry to the order of $\pm 0.5\%$. Theoretical estimates of the asymmetry based mainly on π^0 - η mixing are about 0.1%.

Pedroni *et al.*² made a direct comparison of $\pi^\pm d$ total cross sections. They performed a classical transmission experiment with pions ranging in energy from 70 to 370 MeV and with statistical accuracies of about 2%. They found significant and systematic differences between π^-d and π^+d total cross sections as a function of pion energy. The difference between these cross sections after Coulomb and other electromagnetic corrections should be zero. It was found that, after Coulomb corrections, the π^+d total cross section is larger than the π^-d total cross section in the energy region below the 3-3 resonance (180 MeV). The difference reached a maximum of 2–4 mb (out of 175 mb) near 140 MeV. The π^-d total cross section was found to be larger in the region above the 3-3 resonance and reached a 4–6 mb excess (out of 140 mb) near 250 MeV. Pedroni *et al.*² parametrized residual differences, indicative of charge asymmetry, in terms of mass and width differences among the components of the Δ isobar. These corrections will be discussed in detail in Sec. IV.

There have been several measurements of π^+d differential cross sections,^{7,51-57} and even a phase shift analysis⁴⁰ of these data, but no accurate π^-d differential cross section measurements.^{6,57} Prior to the present measurements there was only one experiment⁵⁸ which measured (in emulsions, with very poor statistics) both π^+d and π^-d differential cross sections at the same energy. There has since been one 65 MeV $\pi^\pm d$ comparison.⁵⁹ The recent tensor polarization measurements of Holt *et al.*³⁷ have also given differential cross section values at 180° at the same energy for both π^+d and π^-d scattering. The present measurements constitute the first good statistics π^-d angular distributions and the first accurate comparison of π^+d and π^-d differential cross sections in this energy region.

The presence of the electromagnetic interaction introduces several small corrections in the analysis of the difference between π^+d and π^-d differential cross sections. The Rutherford elastic scattering cross sections are the same for both π^+d and π^-d . The Coulomb-nuclear interference terms differ for π^+d and π^-d and depend on the purely hadronic phase shift δ_S and these terms, along with Coulomb phase terms which enter directly into the scattering amplitude, produce small differences in π^+d and π^-d differential cross sections. The method for extracting these differences is described in general by Plessas, Streit, and Zingl,⁶⁰ and in particular for the πd system by Thomas.⁹ A positive pion entering the strong field near the deuteron will have a slightly lower energy than a negative pion with the same free space incident energy. This change in effective interaction energy also affects the strong interaction cross sections. Finally, mass and width differences among the components of the intermediate Δ resonance in the pion-nucleon system can give rise to small differences between π^+d and π^-d scattering which are explicitly charge asymmetric. Each of these effects is discussed in detail in Sec. IV.

III. EXPERIMENTAL PROCEDURES

The experiment was performed at the Energetic Pion Channel and Spectrometer (EPICS) facility of the Clinton P. Anderson Meson Physics Facility (LAMPF). The mean incident pion energy was 143 MeV (245 MeV/ c). This energy was chosen because (1) the data of Pedroni *et al.*² indicated a maximal deviation from charge symmetry at this energy, (2) the Bussey *et al.*⁵ comparison $\pi^\pm p$ data were measured at approximately 143 MeV, and (3) the Schweizerisches Institut für Nuklearforschung

(SIN) π^+d measurements of Gabathuler *et al.*⁷ were made at 143 MeV. The full momentum acceptance of the channel ($\pm 1\%$) was used for all π^+ and π^- data runs. For the π^+ beam the channel acceptance in the horizontal scattering plane was reduced to minimize count rate effects at forward angles. This reduced acceptance was used for the entire angular range of this experiment to ensure a consistent set of data. Additional data were also taken at some of the larger angles with several different horizontal acceptances to verify that the data were independent of the channel acceptance in the horizontal scattering plane. With an average proton production beam of 550 μA , the incident π^- beam intensity was 2×10^7 pions/sec while the π^+ beam intensity was 3×10^7 pions/sec with the reduced acceptance.

The pion flux was monitored with two ion chambers in the pion beam approximately 0.7 m behind the scattering target and one in the primary proton beam just upstream of the pion production target. A 4.5 cm thick carbon block was placed in front of the pion beam ion chambers to remove protons. All flux monitors agreed within $\pm 1\%$. At the furthest forward angle (21°) the ion chambers interfered with the scattered beam and were moved to the side. These short runs were taken with only the primary proton beam current monitor to determine the pion flux.

An in-beam time-of-flight spectrometer sampled the incident beam phase space to give the relative number of pions, muons, and electrons within a 5 nsec beam burst. The system consisted of two fast Pilot U scintillators separated by 4.5 m and placed in the direct pion beam after the target and ion chambers. The scintillators were mounted on RCA C31024 photomultiplier tubes and fast timing techniques were used to determine the time-of-flight between the scintillators. The inherent resolution of the entire system was 190 psec, quite adequate to give clean separation of π 's, μ 's, and e 's within a 5 nsec beam burst. Analysis of the time-of-flight spectrum provided a monitor of the pion content of the beam and runs in which the pion fraction differed from the mean by more than 1% were rejected. Such deviations could be caused by the wandering of the proton beam on the pion production target. The location of the proton beam on the production target was therefore also monitored periodically. Measurements indicate that a shift of more than 3 mm produced a 2–3% change in the pion fraction of the EPICS beam. Runs in which the position of the proton beam differed from the mean by more than 1 mm were rejected.

The only part of this experiment sensitive to these changes was during the short time required for a hydrogen normalization for a deuterium measurement at the same angle. Here a change in the pion fraction could affect the number of incident pions without significantly changing the ion chamber reading. The observed long term (several day) stability of the beam and of the pion fraction was very good. Typical variations were <0.3 mm and $<0.5\%$, respectively, and a few runs were rejected for variations larger than this.

Very few data points were rejected for any of the above reasons. One additional data set, at $\theta_{\text{lab}}=120^\circ$, was rejected in spite of agreeing reasonably well with the other asymmetry data because the spectrometer was almost touching the EPICS area wall, which had not at that time been well shielded, and background rates were high.

The scattering targets were CD_2 (194 mg/cm^2), CH_2 (152.7 mg/cm^2), and C (131.5 mg/cm^2). The isotopic purity of the deuterium in the CD_2 target was $>99\%$. The thicknesses were determined by measuring the masses and areas. Micrometer measurements indicated uniformity to within $\pm 1\%$. The target sizes were approximately $15 \text{ cm} \times 23 \text{ cm}$, larger than the nominal beam size of $10 \text{ cm} \times 20 \text{ cm}$. The targets were reproducible in position to within 0.01 cm . The angle of the target with

respect to the incident beam was determined and reproducible to within $\pm 0.05^\circ$, and was consistently set at half the scattering angle. The energy loss of a 143 MeV pion normally incident on the CD_2 target was about 400 keV . Mean scattering energies are listed in Table I for each angle.

Data collected with the CD_2 target were normalized to data collected immediately thereafter with the CH_2 target. Differential pion absorption between CD_2 and CH_2 targets could possibly affect the relative ion chamber readings for the two sets of data. The total, elastic, inelastic, charge exchange, radiative absorption, and capture cross section data of Richard-Serre *et al.*⁶¹ were used to calculate pion removal by CD_2 and CH_2 targets. For the worst case (spectrometer at 115° , target angle 57.5° , π^-) the percentages of pion removed from the beam are 0.24 and 0.05% , for the two targets, respectively. Thus absorption corrections are negligible in this particular experiment.

Scattered pions were detected with the spectrometer and data acquisition system of the EPICS facility.⁶² Spectrometer delay line drift chamber efficiencies were measured by requiring that the drift times in each plane (there were 16 planes) be within a nominal $80 \mu\text{sec}$. Multiple track events were eliminated by requiring that the positions determined in adjacent planes be within 1 mm of each

TABLE I. Differential cross sections and uncertainties for $\pi^\pm p$ elastic scattering used in the present analysis as calculated from the SCATPI (Ref. 63) program. The errors are those given by the program. Target thickness $\text{CH}_2=0.1527 \text{ g/cm}^2$; stopping power $=2.357 \text{ MeV g/cm}^2$.

θ_{lab}	θ_{tgt}	$\frac{1}{2} \frac{\Delta E}{\cos\theta_{\text{tgt}}}$ (MeV)	E_{mean} (MeV)	$\pi^+ p$ $\frac{d\sigma}{d\Omega} \left[\frac{\text{mb}}{\text{sr}} \right]$	$\pi^- p$ $\frac{d\sigma}{d\Omega} \left[\frac{\text{mb}}{\text{sr}} \right]$
21.4°	10.7°	0.183	142.82	26.297±0.098	4.814±0.051
28.0°	14.0°	0.186	142.81	23.360±0.081	3.896±0.038
35.0°	17.5°	0.189	142.81	19.673±0.064	3.121±0.029
43.4°	21.7°	0.194	142.81	15.370±0.050	2.372±0.021
50.0°	25.0°	0.199	142.80	12.498±0.045	1.838±0.017
56.0°	28.0°	0.204	142.80	10.448±0.044	1.470±0.015
60.0°	30.0°	0.208	142.79	9.402±0.044	1.271±0.014
62.0°	31.0°	0.210	142.79	8.977±0.043	1.185±0.013
70.0°	35.0°	0.220	142.78	7.886±0.042	0.922±0.012
72.0°	36.0°	0.222	142.78	7.754±0.042	0.875±0.011
80.0°	40.0°	0.235	142.77	7.698±0.039	0.749±0.010
90.0°	45.0°	0.254	142.75	8.423±0.034	0.700±0.009
97.0°	48.5°	0.272	142.73	9.247±0.032	0.712±0.009
100.0°	50.0°	0.280	142.72	9.642±0.031	0.724±0.009
111.5°	55.8°	0.320	142.68	11.230±0.033	0.796±0.009
115.0°	57.5°	0.335	142.66	11.701±0.035	0.821±0.009
120.0°	60.0°	0.360	142.64	12.345±0.038	0.857±0.009

other. The system fast trigger was the coincidence of signals in entrance wire chambers and focal plane scintillators. All singles rates in all chambers and scintillators were monitored and a few runs with anomalous rate ratios were discarded. Computer live times were as small as 30% at the most forward scattering angles. They were accurately determined by reducing the incident pion flux until a constant yield was obtained, and data were collected only in this region of constant yield.

Data for the $\pi^\pm p$ reaction were obtained at every scattering angle. These data were normalized to the differential cross section measurements of Bussey *et al.*⁵ and to theoretical $\pi^\pm p$ cross section calculations determined with the computer program SCATPI (Ref. 63) from the $\pi^\pm p$ phase shifts of Carter *et al.*⁶⁴ (see below) to determine the incident pion flux and effective solid angle of the spectrometer.

The angular range covered by this experiment was $22^\circ \leq \theta_{\text{lab}} \leq 120^\circ$. The forward angle was limited by forward scattered protons and the resultant rates in the first chambers, while the maximum angle was defined by the point at which the spectrometer hit the wall of the experimental area. The angular resolution of the spectrometer system was 0.5° , determined by the angular divergence of the incident beam in the scattering plane. Kinematic shift comparisons of elastic scattering from ^{12}C and ^1H showed the absolute scattering angle to be within 0.1° of the setting determined from the spectrometer floor angle. This angular resolution was particularly important because of the rapid kinematic variation of the cross sections.

A full kinematic calculation was done for each event through the spectrometer and missing mass was histogrammed. The system resolution of 400 keV was dominated by the angular resolution and straggling in the exit window of the scattering chamber and the entrance window of the spectrometer.

Software projections were made back to the scattering target and events outside accepted ranges were eliminated. Muons scattered from the beam by the target were not eliminated but are expected to be few even at the most forward angles and cancel in the cross section ratio. Pions decaying in the 5 m between the scattering target and the wire chambers in front of the spectrometer dipoles were also not eliminated. For elastic scattering they provide a small and continuous background which cancels out exactly in the $\pi^\pm d$ cross section ratios. For muons from pion decay within the dipoles, the angles of the event in the wire chambers were compared with those calculated from the focal plane

wire chamber information. Angles outside a ± 10 mrad difference were eliminated and said to be from forward decaying pions.

Data were collected in angular bins corresponding to the 1° , 3° , and the full angular acceptance of the spectrometer. We used the 3° angular acceptance bins for cross section determinations and the full acceptance bins for consistency checks.

At each angle, the magnetic fields of the spectrometer dipoles were cycled as necessary and set to the value required to put pions scattered from deuterium at the center of the focal plane. A nuclear magnetic resonance (NMR) Gaussmeter was used to set the dipole fields. Data were then collected for both the CD_2 and carbon targets for π^+ or π^- scattering. The fields of all spectrometer elements were then lowered to the value required to put pions scattered from hydrogen consistently at the center of the focal plane to remove any uncertainty in the spectrometer acceptance. Data were then collected for both the CH_2 and C targets at this field setting. The currents through all elements were then reversed and the magnets cycled to minimize hysteresis effects. With the aid of the NMR Gaussmeter, channel, and spectrometer, dipole magnetic fields were set to within ± 0.3 G of their previous magnitudes for π^+ scattering. The same data collection procedures were then repeated for π^- scattering. Since the channel field was 10.7 kG, a change of even 1 G, which corresponds to a change in kinetic energy of 20 keV, changes the πp comparison cross sections by less than 0.05% at the smallest angle measured (worst case) and less than 0.03% at 90° . These effects and also the effect of the change in the spectrometer acceptance due to dipole field variations are thus completely negligible in this experiment.

The exact reversal of all magnetic fields without any other experimental configuration changes and the temporal juxtaposition of π^+ and π^- data collection reduced many systematic uncertainties and effects of long term fluctuations. Data collected with the carbon target enabled background subtraction for both the CD_2 and the CH_2 targets. The resolution of the EPICS spectrometer was particularly useful in making this subtraction reliable. This procedure also eliminated any interference from inelastic states in carbon with the tails of the deuteron elastic peak. Background subtraction was done both by normalizing charge collected and by equating areas in the exclusively carbon scattering regions of the spectra. These methods were consistent. A typical spectrum before and after background subtraction is shown in Fig. 1.

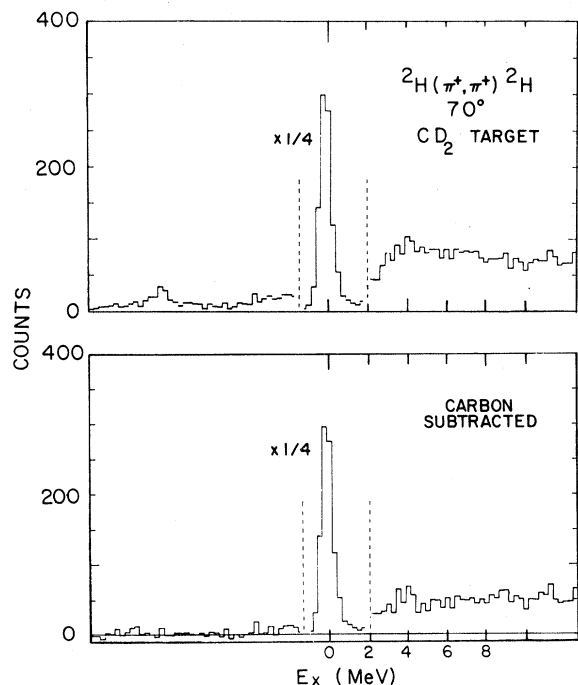


FIG. 1. Missing mass spectrum for 143 MeV π^+ elastic scattering from deuterium at $\theta_{\text{lab}} = 70^\circ$. The top part of the figure shows raw data taken with the CD_2 target while the lower part shows the data after subtraction of the carbon background.

The central 3° angular range in the scattering plane was used in the data presented in Fig. 1. Peak areas were obtained by using consistent energy bins for both π^+ and π^- . Uncertainties include statistics in the resultant peak areas and in the background used in the subtraction.

The data are normalized with the $\pi^\pm p$ differential cross sections calculated with the SCATPI phase shift code,⁶³ based on the $\pi^\pm p$ phase shifts determined by Carter, Bugg, and Carter.⁶⁴ This set of phase shifts was strongly influenced by the accurate $\pi^\pm p$ data of Bussey *et al.*⁵ and was determined by independent fitting of $\pi^+ p$ and $\pi^- p$ data, thus explicitly allowing charge dependent $\pi^\pm p$ phase shifts. These data are also statistically the best $\pi^\pm p$ cross section measurements made to date, and consequently strongly influence all $\pi^\pm p$ phase shift determinations. The differential cross sections calculated with SCATPI agree with the Bussey *et al.*⁵ data at this energy within 2% for $\pi^+ p$ and 2.5% for $\pi^- p$.

There are many other sets of $\pi^\pm p$ phase shifts and they vary over a wide range in their predictions of $\pi^\pm p$ differential cross sections at this energy. Phase shifts determined from combined $\pi^+ p$ and $\pi^- p$ data are not appropriate for the present

analysis as they build in isospin invariance. An explicit comparison of $\pi^\pm p$ differential cross sections determined from the charge independent Carnegie-Mellon University—Lawrence Berkeley Laboratory (CMU-LBL),⁶⁵ Rowe-Salomon-Landau,⁶⁶ and Karlsruhe⁶⁷ phase shift solutions with the charge dependent Virginia Polytechnic Institute (VPI) (Ref. 68) and Carter-Bugg-Carter⁶⁴ solutions is given in Appendix A.

The VPI phase shifts⁶⁸ were found from independent analysis of $\pi^+ p$ and $\pi^- p$ data. They differ significantly from the SCATPI analysis in that they predict cross sections that are several percent lower at all angles, and the total cross sections predicted are 3–4% lower than observed by Pedroni. The SCATPI total cross section calculations, on the other hand, are 3–4% higher than observation.

In view of possible differences, discussed in Appendix A, between these and future $\pi^\pm p$ phase shift analyses and data, we have listed in Table I the cross sections and uncertainties of the $\pi^\pm p$ cross sections used in the present analysis. The $\pi^\pm p$ cross sections listed include Coulomb scattering and these Coulomb scattering contributions are accurate to better than 1%. The mean scattering energy is altered slightly by the energy loss of the incident pions, which changes with the angle of the target in the pion beam; we have therefore also listed the mean energy.

Differential cross sections were calculated from the relationship:

$$\left. \frac{d\sigma}{d\Omega} \right|_{d,c.m.} = \frac{C_d N_d J_d}{C_p N_p J_p} \left. \frac{d\sigma}{d\Omega} \right|_{p,c.m.} 2 \frac{\frac{2}{14} \rho(\text{CH}_2)}{\frac{4}{16} \rho(\text{CD}_2)}, \quad (3.1)$$

where C is the integrated number of counts observed, J is the Jacobian for the laboratory to c.m. transformation, the subscripts p and d refer to proton and deuterium scattering, respectively, N is the normalization factor which is dependent on the integrated flux in the beam monitor, wire chamber efficiency and computer live time, ρ is the target thickness, and

$$\left. \frac{d\sigma}{d\Omega} \right|_{p,c.m.}$$

is the c.m. cross section for πp scattering from the SCATPI phase shift program.⁶³

Differential cross sections for both $\pi^+ d$ and $\pi^- d$ are shown in Fig. 2 and tabulated in Table II. The errors include statistics of foreground and background areas from CD_2 , CH_2 , and C targets and the uncertainty in the $\pi^\pm p$ differential cross sections as

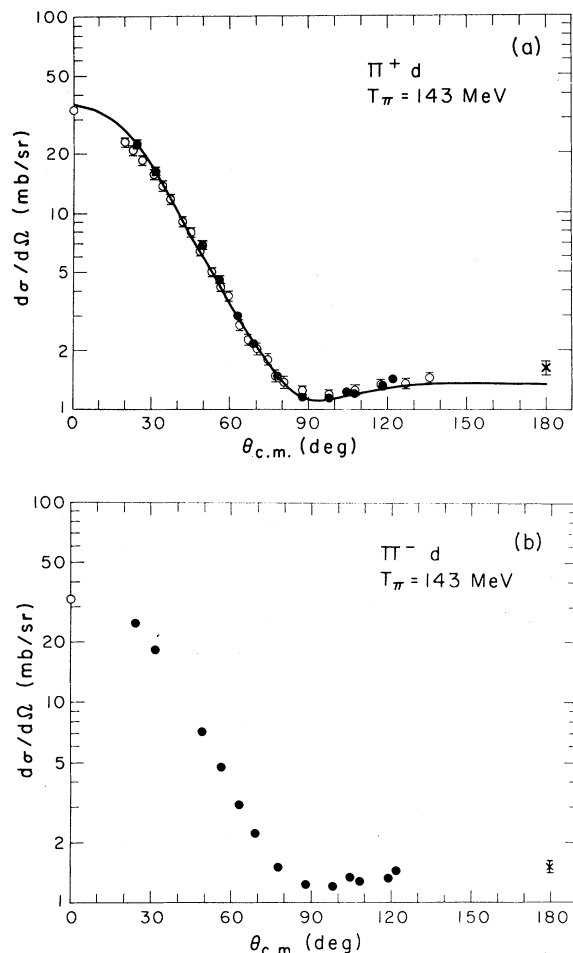


FIG. 2. Differential cross sections for $\pi^\pm d$ elastic scattering. The solid points are our results. In the upper part of the figure, the π^+ data of Gabathuler *et al.* (Ref. 7) (open circles), the 180° data point of Holt *et al.* (Ref. 37), and the 0° data point from the total cross section data of Pedroni *et al.* (Ref. 2) are also presented. The curve is a three-body calculation of Giraud *et al.* (Ref. 8). The lower part of the figure shows our $\pi^- d$ differential cross sections as well as the 180° point from Holt *et al.* and the 0° point from Pedroni *et al.*

given by the SCATPI program. The use of a different set of $\pi^\pm p$ phases could alter the absolute value of the differential cross sections by several percent. We have used this set in order to compare with the data of Gabathuler *et al.*⁷ which are based on the same $\pi^\pm p$ phase shifts. Also shown in Fig. 2 are the $\pi^+ d$ differential cross section data measured by Gabathuler *et al.*⁷ at 143 MeV, and the agreement with our data is very good. The 0° points shown are from the total cross section measurements of Pedroni *et al.*² and the 180° points are from the tensor polarization measurements of Holt

*et al.*³⁷ Also shown in Fig. 2 is the three-body πd calculation of Giraud *et al.*⁸ which is fully relativistic and includes all pion-nucleon S and P wave amplitudes. The agreement with our data is excellent.

The ratio of the difference between $\pi^- d$ and $\pi^+ d$ cross sections to the sum [Eq. (1.1)] is the parameter used to describe deviations from charge symmetry. The ratio measurement is much more precise than the differential cross section measurements themselves as many uncertainties cancel. In particular, uncertainties due to target thickness, pion decay, dead time corrections, and count rate effects are essentially eliminated in the ratio measurement.

The asymmetry data are shown in Fig. 3. No corrections, Coulomb or otherwise, are included in this figure. The errors shown include both statistics and the tabulated (Table I) uncertainties in the $\pi^+ p$ cross sections. All asymmetry ratios are the result of correlated data sets in which π^+ and π^- data were collected immediately after one another to reduce any systematic effects which might vary slowly with time. Measurements repeated at the same angle at a later time are represented as separate data points. Except for one point at 108° where the initial measurements had poor statistics and large error bars, the repeatability was excellent. The sharp increase at forward angles is expected from Coulomb effects which will enhance the $\pi^- d$ yield relative to the $\pi^+ d$ yield at small angles. Back angle data are close to zero except for a possible bump near 100°. This indicates conservation of charge symmetry to zeroth order before consideration of known corrections.

The curves shown in Fig. 3 represent three body calculations of the A_π asymmetry ratio for various sets of πd phase shifts. Coulomb and Coulomb-nuclear interference contributions have been included in the calculation. The solid line includes all S - and P -wave pion nucleon amplitudes, 4% D state in the deuteron, no absorption, and is fully relativistic. It is the basis for corrections discussed later in this paper. The effect on the asymmetry of the inclusion of more deuteron D state or true pion absorption is seen to be small. The dashed-dotted-dashed curve is the same as the solid one except for a 6.7% deuteron D state while the dashed-dotted-dashed curve includes pion absorption. These πd phases are from Rinat *et al.*¹² The dotted curve is from the phase shifts of Blankleider and Afnan³⁴ and the dashed curve treats the interaction as entirely due to the P_{33} πN amplitude. All calculations shown here explicitly assume charge symmetry.

TABLE II. Measured $\pi^\pm d$ differential cross sections and asymmetry ratios for $\pi^\pm d$ elastic scattering at 143 MeV.

$\theta_{c.m.}$ (deg)	$d\sigma/d\Omega$ (mb/sr) ^a		A_π^b
	π^+d	π^-d	$\frac{\sigma_-(\theta) - \sigma_+(\theta)}{\sigma_-(\theta) + \sigma_+(\theta)}$
24.4	22.68±1.00	25.00±0.60	0.048±0.030
31.8	16.16±0.55	17.36±0.34	0.036±0.022
49.1	6.78±0.25	7.08±0.22	0.022±0.013
	7.12±0.24	7.24±0.22	0.009±0.013
56.2	4.60±0.08	4.70±0.15	0.011±0.014
62.6	2.98±0.05	3.10±0.08	0.021±0.011
69.0	2.19±0.04	2.23±0.06	0.008±0.011
	2.16±0.04		0.015±0.011
77.4	1.50±0.03	1.51±0.04	0.003±0.008
	1.43±0.03	1.49±0.04	0.020±0.008
87.7	1.16±0.03	1.23±0.03	0.029±0.012
97.8	1.11±0.03	1.16±0.03	0.021±0.018
	1.18±0.02	1.25±0.03	0.027±0.012
104.6	1.23±0.03	1.33±0.03	0.036±0.012
107.6	1.16±0.04	1.30±0.05	0.056±0.021
	1.24±0.02	1.26±0.02	0.007±0.012
118.6	1.31±0.03	1.31±0.03	0.003±0.014
121.9	1.42±0.03	1.44±0.05	0.007±0.020

^aDifferential cross section errors include all statistical errors in πd and πp measurements as well as πp systematic errors as calculated by the SCATPI phase shift program. The second set of values indicated for cross sections and asymmetry at 77.4°, 97.8°, 107.6°, and (only value) at 121.9° are from measurements made at several different times up to 1 year after the original measurements.

^bAsymmetry ratio errors include πd statistical errors, πp systematic errors, and extremal errors from the ratio of πp yield to $\sigma_{\pi p}$ (SCATPI) fit over all angles. No radiative corrections are included in this table.

There can be a systematic error associated with the use of different $\pi^\pm p$ phase shifts. The only other sets of $\pi^\pm p$ phases which do not explicitly assume isospin invariance are the VPI A1 (π^+p) and B1 (π^-p) solutions.⁶⁸ All of our A_π asymmetry ratio data have been recalculated using these phases and the results are compared with A_π data based on the Carter, Bugg, and Carter⁶⁴ phases in Fig. 4. The A_π values are systematically lower but always within approximately 0.01 of the original data. Thus referenced to a median value there is a ± 0.005

systematic uncertainty in the ratio data associated with the use of different $\pi^\pm p$ phase shifts.

IV. CORRECTIONS AND DISCUSSION

In this section electromagnetic corrections affecting experimental data and the theoretical calculations of differences between π^+d and π^-d elastic scattering are discussed.

The only electromagnetic correction applied to

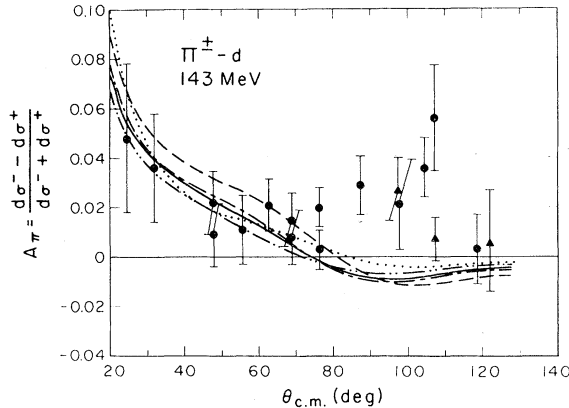


FIG. 3. The A_π asymmetry data represent the difference between π^-d and π^+d elastic scattering differential cross sections divided by the sum. Data points indicated by triangles depict measurements made at a later time. No corrections for radiative or Coulomb effects have been included. Theoretical curves represent three-body calculations of the asymmetry for various sets of πd phase shifts after subtraction of Coulomb and Coulomb-nuclear interference contributions to the cross sections. The solid line includes all S and P wave πN amplitudes, 4% D state in the deuteron, no absorption, and is relativistic. It is the basis of corrections discussed later in this paper. The dashed-dotted-dashed curve is the same except for a 6.7% deuteron D state while the dashed-dotted-dotted-dashed curve includes pion absorption. These phase shifts are from Rinat *et al.* (Ref. 12). The dashed curve includes only the P_{33} πN amplitude while the dotted curve is from the phase shifts of Blankleider and Afnan (Ref. 34). All calculations assume charge symmetry.

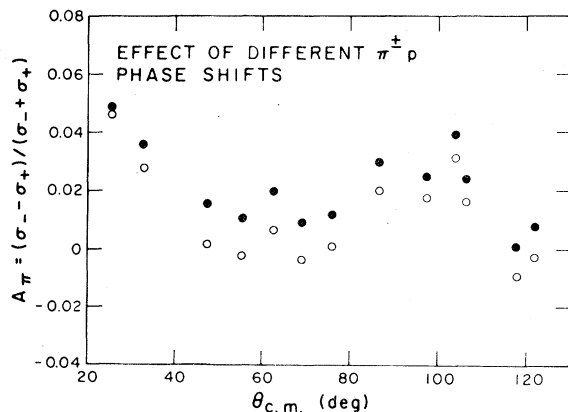


FIG. 4. Effect of different π^+p phase shifts on averaged asymmetry data points. The use of the VPI charge dependent phase shifts (Ref. 68) (open circles) instead of the Carter, Bugg, and Carter (Ref. 64) (solid circles) ones would cause an average downward shift in the asymmetry data of 0.009.

the experimental data is the radiative correction caused by photons emitted during pion scattering. Electromagnetic processes affecting theoretical calculations include Coulomb-nuclear interference in scattering amplitudes, and the effective interaction energies for π^+d and π^-d scattering at the surface of the deuteron due to the respective repulsive and attractive Coulomb fields. Finally, the effect of mass differences among the components of the intermediate Δ isobar is calculated.

A. Radiative corrections

Bremsstrahlung radiation causes a low energy tail on peaks and results in loss of counts from the integrated total number of scattered pions for a given energy acceptance. Radiative corrections to the differential cross sections were calculated from the relationships given by Borie.⁶⁹ The effects differ for π^+ and π^- scattering and for scattering from deuterium and hydrogen. The values of the corrections to the differential cross sections and to the A_π ratio are listed in Table III. The π^+d radiative correction calculations used an experimental peak integration which extended 1.7 MeV beyond the central energy while the $\pi^\pm p$ scattering correction calculation used 2.5 MeV. The largest effect is at the largest angle where the asymmetry, A_π , is decreased by approximately 0.007. The error in these corrections due to approximations made in the formulae used in the calculations is less than 10% of the corrections.

B. Coulomb corrections to $\pi^\pm d$ scattering

A great deal of effort has gone into the formal solution of the three-body problem including the Coulomb potential. In the classic three-body system with two charged particles, namely the pd system, the numerical results are still somewhat controversial.⁷⁰⁻⁷⁴ Nevertheless, it does seem that even as low as 10 MeV the Coulomb modification to the strong phase shift is rather small.⁴⁹ We have chosen to treat the Coulomb corrections to the $\pi^\pm d$ system perturbatively for two reasons. First, the exact numerical solution of this three-body problem including a Coulomb potential does not seem possible at the present time. Second, because we are dealing with $Z=1$ and rather high energy, one would *a priori* expect such a treatment to be a good approximation.

From the theory of two-potential scattering we know that the differential cross section (for a spin-

TABLE III. Radiative corrections to $\pi^\pm d$ and $\pi^\pm p$ differential cross sections and asymmetry ratios. The corrections were calculated from equations given by Borie (Ref. 69) and are accurate to better than 10%. Errors in cross sections and in A_π are tabulated in Table II. These corrections are to be added to the data in Table II.

θ_{lab} (deg)	Radiative corrections (mb/sr)				A_π
	$\pi^- d$	$\pi^- p$	$\pi^+ d$	$\pi^+ p$	
21.4	0.003	0.003	0.003	0.002	0.000
28.0	0.007	0.007	0.005	0.004	-0.001
43.5	0.013	0.013	0.010	0.008	-0.001
50.0	0.018	0.018	0.013	0.010	-0.002
56.0	0.020	0.021	0.015	0.011	-0.002
62.0	0.022	0.023	0.016	0.012	-0.003
70.0	0.026	0.028	0.019	0.013	-0.003
80.0	0.031	0.033	0.020	0.015	-0.004
90.0	0.034	0.037	0.023	0.016	-0.005
97.0	0.036	0.039	0.024	0.016	-0.005
100.0	0.038	0.041	0.025	0.016	-0.006
111.5	0.041	0.045	0.026	0.017	-0.006
115.0	0.042	0.047	0.027	0.017	-0.007

less target) is given by the scattering amplitude

$$f(\theta) = f_C(\theta) + f_N(\theta), \quad (4.1)$$

where

$$f_C(\theta) = \frac{\eta}{2k \sin^2(\theta/2)} \times \exp[-i\eta \ln(\sin^2(\theta/2)) + i\pi] \quad (4.2)$$

and

$$f_N(\theta) = \sum_l (2l+1) e^{2i(\sigma_l - \sigma_0)} \times \frac{e^{i\delta_l} \sin \delta_l}{k} P_l(\cos \theta). \quad (4.3)$$

The Coulomb parameter $\eta = Ze^2/hv$ (for the pion the relative velocity v is calculated relativistically) and the Coulomb phases σ_l are defined by

$$\sigma_l = \arg \Gamma(l+1+i\eta). \quad (4.4)$$

Note that the strong amplitude f_N explicitly involves the Coulomb phases σ_l .

The differential scattering cross sections calculated with Eq. (4.1) will have terms arising from the strong amplitude f_N , the Coulomb amplitude f_C , and a Coulomb-nuclear interference term involving both f_C and f_N . The purely Coulomb contribution to the cross section is the same for both $\pi^+ d$ and $\pi^- d$ and is easily eliminated. The interference term is slightly dependent on the particular set of three-

body πd phase shifts. These differences were presented in our original analysis¹ for several sets of πd phase shifts ranging from a P_{33} scattering only to a fully relativistic set including all S and P wave pion-nucleon amplitudes as well as absorption. Here we will extract the purely nuclear part of the Coulomb modified strong amplitude.

The phase shifts, δ_l , appearing in the Coulomb modified strong amplitude f_N [Eq. (4.3)] can be written

$$\delta_l = \delta_l^N + \delta_l^{f-s} + \delta_l^{C-N}. \quad (4.5)$$

Here δ_l^N is the strong phase shift obtained without any Coulomb effects at all, and δ_l^{f-s} is the correction to the point Coulomb phase shift σ_l because of the charge distribution of the target. To lowest order in α we can multiply $f_C(\theta)$ by the deuteron form factor $[F_d(q/2)]$ and set δ_l^{f-s} equal to zero; this is done here. Finally, δ_l^{C-N} is the correction to the strong phase shift δ_l^N arising from the quantum mechanical interference between the Coulomb and nuclear potentials. The only way to determine δ_l^{C-N} exactly is to solve the full problem. However, a number of approximation techniques have been suggested.

In the first analysis¹ of the 143 MeV $\pi^\pm d$ data the phase δ_l^{C-N} was set equal to zero, and only the model independent Coulomb effects were included. The generalization to scattering from a spin-one target was achieved following Ref. 9. The strong phase shifts δ_{lj} were taken from a recent three-body calculation by Rinat *et al.*¹² and the off-diagonal

amplitudes $f_{l',l}^j$ ($l' \neq l$) were omitted. (The latter approximation has been proven to be excellent for differential cross sections.¹²) In this work we also use the πd amplitudes of Blankleider and Afnan,³⁴ in order to test the model dependence of the analysis. However, the most significant change in this work is our inclusion of δ_l^{C-N} .

We have chosen to estimate δ_l^{C-N} by the simple and intuitively reasonable approximation of evaluating the π^+ and π^- phases at an energy below and above the incident energy by the Coulomb energy at the surface of the deuteron, namely 0.75 MeV at 1.92 fm. (A similar estimate was made by Myhrer and Pilkuhn³ in their study of the $\pi^\pm d$ total cross section difference.) Although there are more sophisticated schemes they should not differ significantly for the π - d system. For example, Germond and Wilkin⁷⁵ suggest using

$$\delta \left[E_l - V_C \left(\frac{l + \frac{1}{2}}{k} \right) \right]$$

on the basis of an eikonal model. This is in essential agreement with our simple prescription because our major correction comes in the p wave and is of the order 1–1.5%; even less correction comes in more peripheral waves. Finally, the change in the πd amplitude when the energy was changed by ± 0.75 MeV was calculated by assuming a Breit-Wigner shape for each πd partial wave amplitude.

The change in the elastic scattering matrix element $\tau_l(E)$ is given by (see Appendix B)

$$\Delta\tau_l(E) = \left[\frac{2\delta E_l}{\Gamma_{el}^l} \tau_l(E) + \frac{(3+a^2k^2)}{(1+a^2k^2)} \frac{\omega_k \delta E_l}{k^2} \left\{ 1 + i \frac{\Gamma^l}{\Gamma_{el}^l} \tau_l(E) \right\} \right] \tau_l(E), \quad (4.6)$$

where

$$\omega_k = (k^2 + m_\pi^2)^{1/2},$$

$a = 1.15$ fm, Γ and Γ_{el} are the total and elastic widths, and δE_l is the small shift in the effective interaction energy in channel l . These small changes in the πd matrix elements were then used to generate a new set of $\pi^\pm d$ differential cross sections. The effect of a constant shift $\delta E_l = \pm 0.75$ MeV for $\pi^\pm d$ on the calculated asymmetry is shown as the dashed line in Fig. 6. (See below.) The asymmetry is shifted upwards at all angles as expected for an incident pion energy less than the 3-3 resonance energy of 180 MeV. The shift is approximately 0.015 at small angles and increases to 0.02 at 120°.

C. Effect of charge symmetry violation on πd scattering

In this section we consider the charge symmetry violating contributions expected from π^\pm scattering from a spin 1 deuteron due to mass and width differences among the components of the Δ isobar. The rotation of the isospin vector about the y axis should not change masses of particles corresponding to the T_3 projection of the isospin. That this charge symmetry does not hold exactly is seen from the mass difference $m_n - m_p = 1.3$ MeV, which is in the opposite direction to that expected from Coulomb effects and implies different masses for u and d quarks. Similar effects are to be expected for

the four-component Δ isobar system, and this experiment provides a direct indication of their magnitude.

In the impulse approximation the scattering amplitude of a pion from a deuteron can be written as

$$f_{\pi d}(\theta) = [f_{\pi p}(\theta) + f_{\pi n}(\theta)] F_d(\theta), \quad (4.7)$$

where F_d is the deuteron form factor. The pion nucleon scattering amplitudes $f_{\pi N}$ can be expressed in terms of charge symmetric isospin $\frac{3}{2}$ and $\frac{1}{2}$ amplitudes⁷⁶ plus a charge symmetry violating term ϵ :

$$\pi^+ p: f_{\pi^+ p} = f_{3/2} + \epsilon_{++}, \quad (4.8a)$$

$$\pi^+ n: f_{\pi^+ n} = \frac{1}{3}(f_{3/2} + 2f_{1/2} + \epsilon_{+-}), \quad (4.8b)$$

$$\pi^- p: f_{\pi^- p} = \frac{1}{3}(f_{3/2} + 2f_{1/2} + \epsilon_{-+}), \quad (4.8c)$$

$$\pi^- n: f_{\pi^- n} = f_{3/2} + \epsilon_{--}. \quad (4.8d)$$

The charge symmetry violating terms ϵ_{++} , ϵ_{+-} , ϵ_{-+} , and ϵ_{--} are related to the Δ^{++} , Δ^+ , Δ^0 , and Δ^- components of the Δ isobar, respectively.

The isospin amplitudes can be written for both spin-flip (F) and non-spin-flip (NF) amplitudes, and their sum is incoherent. If we restrict ourselves to S and P wave scattering, then these amplitudes can in turn be expressed⁷⁷ in terms of partial wave scattering amplitudes $a_{L2T,2J}$:

$$f_{\text{NF}}(\frac{3}{2}) = \frac{1}{k} [a_{S_{31}} + (2a_{P_{33}} + a_{P_{31}}) \cos\theta], \quad (4.9a)$$

$$f_F(\frac{3}{2}) = \frac{1}{k} [(a_{P_{31}} - a_{P_{33}}) \sin\theta e^{i\phi}], \quad (4.9b)$$

$$f_{\text{NF}}(\frac{1}{2}) = \frac{1}{k} [a_{S_{11}} + (2a_{P_{13}} + a_{P_{11}}) \cos\theta], \quad (4.9c)$$

$$f_F(\frac{1}{2}) = \frac{1}{k} [(a_{P_{11}} - a_{P_{13}}) \sin\theta e^{i\phi}], \quad (4.9d)$$

where k is the c.m. momentum. Each complex partial wave scattering amplitude $a_{L_{2T,2J}}$ is determined from

$$a_{L_{2T,2J}} = \sin\delta_{L_{2T,2J}} e^{i\delta_{L_{2T,2J}}}, \quad (4.10)$$

where $\delta_{L_{2T,2J}}$ is the L th partial wave πN phase shift for isospin T and total angular momentum J .

Neglecting charge symmetry violating terms, the amplitude for πd scattering is given by

$$f_{\pi d} = f_{3/2} + \frac{1}{3}(f_{3/2} + 2f_{1/2}). \quad (4.11)$$

The cross section for unpolarized πd scattering is thus

$$\sigma_{\pi d} = \frac{16}{9} \left\{ |f_{3/2}|^2 + \frac{1}{4} |f_{1/2}|^2 + \text{Re}(f_{3/2}^* f_{1/2}) \right\}, \quad (4.12)$$

where

$$|f_{3/2}|^2 = |f_{\text{NF}}(\frac{3}{2})|^2 + \frac{2}{3} |f_F(\frac{3}{2})|^2, \quad (4.13a)$$

$$|f_{1/2}|^2 = |f_{\text{NF}}(\frac{1}{2})|^2 + \frac{2}{3} |f_F(\frac{1}{2})|^2, \quad (4.13b)$$

and

$$f_{3/2}^* f_{1/2} = f_{\text{NF}}^*(\frac{3}{2}) f_{\text{NF}}(\frac{1}{2}) + \frac{2}{3} f_F^*(\frac{3}{2}) f_F(\frac{1}{2}). \quad (4.13c)$$

The factor of $\frac{2}{3}$ in front of the spin-flip terms accounts for the spin-flip transitions allowed for an S state deuteron of spin 1. Transitions possible to that component of the deuteron in a D state have not been incorporated in this approximation. Their effect should be very small since our calculations show that the ratio of spin-flip to non-spin-flip contributions to the πd cross section does not change on increasing the component of the deuteron D state

from 0% to 4%.

Including charge symmetry violating terms, the difference $\Delta\sigma$ between $\pi^- d$ and $\pi^+ d$ elastic scattering is given by

$$\begin{aligned} \Delta\sigma &= |f_{3/2} + \epsilon_{--} + \frac{1}{3}(f_{3/2} + 2f_{1/2} + \epsilon_{--})|^2 \\ &\quad - |f_{3/2} + \epsilon_{++} + \frac{1}{3}(f_{3/2} + 2f_{1/2} + \epsilon_{+-})|^2 \\ &= \frac{8}{3} \text{Re} \left[(f_{3/2}^* + \frac{1}{2} f_{1/2}^*) \right. \\ &\quad \left. \times \{ \epsilon_{--} - \epsilon_{++} + \frac{1}{3}(\epsilon_{--} - \epsilon_{+-}) \} \right], \end{aligned} \quad (4.14)$$

including terms to first order in ϵ .

The charge symmetry violating amplitudes may be estimated in terms of mass and width differences among the components of the Δ by assuming a πN $L = 1$ resonance with a Breit-Wigner (BW) form⁷⁷

$$f_{\text{BW}}(i, \text{NF}) = \frac{W_{0i} \Gamma_{ei}}{(W_{0i}^2 - W^2) - i W_{0i} \Gamma_{ti}} \times \frac{2 \cos\theta}{k}, \quad (4.15a)$$

$$f_{\text{BW}}(i, F) = - \frac{W_{0i} \Gamma_{ei}}{(W_{0i}^2 - W^2) - i W_{0i} \Gamma_{ti}} \times \frac{\sin\theta}{k}, \quad (4.15b)$$

where W_{0i} is the mass of Δ_i , W is the total energy, and Γ_{ei} and Γ_{ti} are the elastic and total widths, respectively. We can express $W_{0i}(\Gamma)$ in terms of an average Δ mass (width) and an isospin dependent correction, $W_{0i} = W_0 + \delta W_i$ and $\Gamma_i = \Gamma_0 + \delta \Gamma_i$. The isospin violating amplitude ϵ is then given by the difference

$$f_{\text{BW}}(W_{0i}, \Gamma_{0i}) - f_{\text{BW}}(W_0, \Gamma_0).$$

Expansion to first order (see Appendix B) in δW and $\delta \Gamma$ gives

$$\Delta f_{0i} = f_{0i} \left[\frac{\delta \Gamma_t}{\Gamma_t} + i f_{0i} \left[\frac{\delta \Gamma_t}{\Gamma_t} + 2i \frac{\delta W}{\Gamma_t} \right] \right], \quad (4.16)$$

where

$$f_{0i} = \frac{W_0 \Gamma_t}{(W_0^2 - W^2) - i W_0 \Gamma_t}. \quad (4.17)$$

The isospin dependent difference can then (see Appendix B) be expressed as

$$\begin{aligned} \epsilon_{--} - \epsilon_{++} + \frac{1}{3}(\epsilon_{-+} - \epsilon_{+-}) \\ = \frac{f_{0t}}{\Gamma_t} (\tilde{C}_{\Gamma_t} + f_{0t}(\tilde{C}_{\Gamma_t} - 2C_W)) \end{aligned} \quad (4.18)$$

and is multiplied by $(2 \cos \theta / k)$ or $(-\sin \theta / k)$, for the spin-flip and non-spin-flip terms, respectively, and where, following Pedroni *et al.*,²

$$C_W = W_{--} - W_{++} + \frac{1}{3}(W_{-+} - W_{+-}) \quad (4.19a)$$

and

$$\tilde{C}_{\Gamma} = \Gamma_{--} - \Gamma_{++} + \frac{1}{3}[\Gamma_{-+} - \Gamma_{+-}]. \quad (4.19b)$$

The masses determined by Myhrer and Pilkuhn³ yield $C_W = 5.5$ MeV. Those determined experimentally by Pedroni *et al.*² give 4.6 ± 0.2 MeV while a quark model calculation by Rubenstein⁷⁸ gives 4.3 MeV, and an MIT bag model calculation of Bickersstaff and Thomas⁷⁹ gives 4.47 MeV. The difference between neutron and proton masses is explicitly included by writing

$$C_W^{\text{eff}} = C_W - \frac{2}{3}(m_n - m_p),$$

reducing the value of C_W by about 0.86 MeV. This constant difference has been incorporated into all our calculations and we will quote values for C_W , not C_W^{eff} , in order to facilitate comparison with other results. The widths are energy dependent,

$$\begin{aligned} \frac{\Delta\sigma}{2\sigma} &= \frac{3}{4} \frac{1}{\Gamma_t} \text{Re}[\tilde{C}_{\Gamma_t} + f_{0t}(i\tilde{C}_{\Gamma_t} - 2C_W)] \\ &= \frac{3}{4} \frac{1}{\Gamma_t} (\tilde{C}_{\Gamma_t}(1 - \text{Im}f_{0t}) - 2C_W \text{Re}f_{0t}). \end{aligned} \quad (4.22)$$

This expression is angle independent and its value at $T_{\pi, \text{lab}} = 143$ MeV is equivalent to a shift in the symmetry ratio of -0.02 for $C_W = 4.35$ MeV. The first term in expression (4.22) is also small (10%) compared to the second and thus the amount of the shift observed in our experimental data can be used to estimate the magnitude of the differences C_W among the Δ masses.

The full expression (4.21) is angle dependent due to the presence of other partial waves. Including both non-spin-flip and spin flip terms and incorporating a factor of $\frac{2}{3}$ for the spin of the deuteron we obtain:

$$\Delta\sigma = \frac{8}{3\Gamma_t} \text{Re} \left\{ [(f_{3/2}^*(\text{NF}) + \frac{1}{2}f_{1/2}^*(\text{NF}))\mathcal{F}] \frac{2 \cos \theta}{k} + \frac{2}{3} [(f_{3/2}^*(F) + \frac{1}{2}f_{1/2}^*(F))\mathcal{F}] \frac{(-\sin \theta)}{k} \right\}, \quad (4.23)$$

where

$$\mathcal{F} = f_{0t} [C_{\Gamma_t} + f_{0t}(iC_{\Gamma_t} - 2C_W)].$$

Evaluation in terms of pion-nucleon amplitudes gives

$$\Gamma_i = \Gamma_{0i} \left[\frac{k}{k_{0i}} \right]^3 \left[\frac{1 + k_{0i}^2 a^2}{1 + k^2 a^2} \right], \quad (4.20)$$

and the mean isospin averaged width thus determined is $\Gamma_0 = 101.6$ MeV, $a = 1.15$ fm, and from (4.19b), $\tilde{C}_{\Gamma} = 1.67$ MeV. The cross section difference is therefore

$$\begin{aligned} \Delta\sigma &= \frac{8}{3\Gamma_t} \text{Re}[(f_{3/2}^* + \frac{1}{2}f_{1/2}^*)f_{0t} \\ &\quad \times \{\tilde{C}_{\Gamma_t} + f_{0t}(i\tilde{C}_{\Gamma_t} - 2C_W)\}] \end{aligned} \quad (4.21)$$

and is again multiplied by

$$\left[\frac{2 \cos \theta}{k} \right]^2$$

or

$$\left[\frac{-\sin \theta}{k} \right]^2$$

for non-spin-flip and spin flip terms, respectively. The magnitude of this effect can be seen to first order by assuming that only the P_{33} amplitude enters Eq. (4.21). In this approximation $(f_{3/2}^* + \frac{1}{2}f_{1/2}^*)$ reduces to $a_{P_{33}}$, which is the same as f_{0t} and

$$\Delta\sigma = \frac{8}{3\Gamma_t} \operatorname{Re} \left\{ \frac{\mathcal{F}}{k^2} [(4a_{P_{33}}^* + 2a_{P_{31}}^* + 2a_{P_{13}}^* + a_{P_{11}}^*) \cos^2\theta + (2a_{S_{31}}^* + a_{S_{11}}^*) \cos\theta + \frac{1}{3}(2a_{P_{33}}^* - 2a_{P_{31}}^* + a_{P_{13}}^* - a_{P_{11}}^*) \sin^2\theta] \right\}. \quad (4.24)$$

Finally, the cross section difference given above is in the pion-nucleon center-of-mass system. An angle transformation is needed to transform to the πd center-of-mass system. The angle transformation applies both to the cross section difference (4.24) and the cross section (4.12) itself and is given by

$$\cos\theta_{\pi N} = \frac{(\alpha^2 + \beta^2) \cos\theta_{\pi d} - 2\alpha\beta}{\alpha^2 + \beta^2 - 2\alpha\beta \cos\theta_{\pi d}}, \quad (4.25)$$

where

$$\alpha = (m + \omega/2)/(m + \omega),$$

$$\beta = \omega/(2(m + \omega)),$$

and

$$\omega = (k^2 + m_p^2)^{1/2}.$$

The calculated differences $\Delta\sigma/2\sigma$ were calculated with the charge independent πN phase shifts of Rowe *et al.*⁶⁶ Note that charge independent phase shifts are required to calculate this correction whereas charge dependent phase shifts were required for the data analysis. The πN c.m. energy used was 115 MeV. The differences $\Delta\sigma/2\sigma$ are plotted in Fig. 5 as a function of the πd c.m.

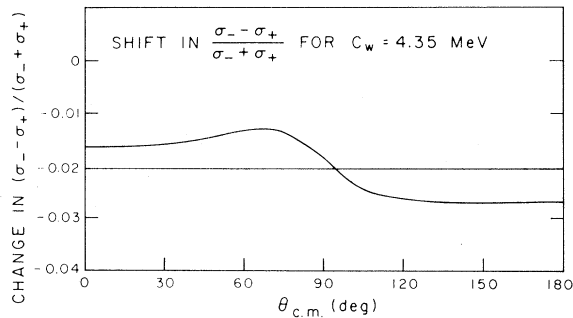


FIG. 5. Charge symmetry violating effects in πd scattering parametrized in terms of mass differences among the components of the delta isobar. The difference $\Delta\sigma$ from Eq. (4.23) divided by 2σ is plotted versus c.m. scattering angle. The C_W parameter is 4.35 MeV. The difference is always negative but somewhat smaller at forward angles than the constant -0.02 expected from a pure 3-3 scattering and somewhat larger at back angles.

scattering angle. The difference is always negative but somewhat smaller at small angles than the -0.02 expected from a pure 3-3 scattering and somewhat larger at back angles.

In Fig. 6 the A_π data, after radiative corrections, are compared to πd three-body calculations including Coulomb-nuclear interference, effective interaction energies (the effect of the Coulomb interaction on the strong phases), and a charge symmetry breaking parameter C_W associated with mass differences among the components of the Δ resonance.

The dashed line in Fig. 6 indicates our calculation with the charge symmetry breaking parameter C_W set to zero. It is obviously in disagreement with our data and clearly shows that charge symmetry is broken in the πd elastic scattering at 143 MeV. This result is to be compared with our original Letter¹ in which no Coulomb energy shift or charge symmetry corrections were included. Theoretical calculations without these Coulomb corrections were in reasonable agreement with our data. The extraction of the pure nuclear amplitude from the Coulomb-modified strong amplitude left us with a result that is incompatible with charge symmetry.

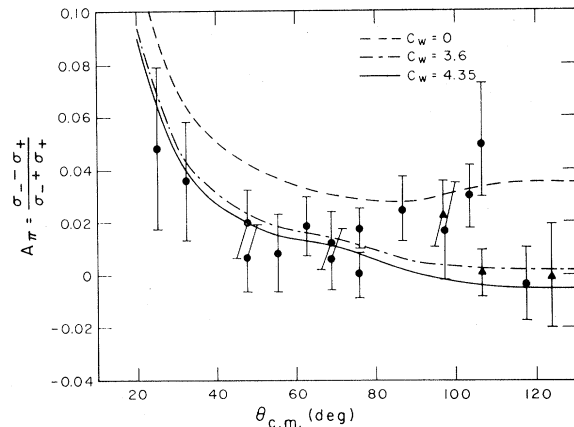


FIG. 6. The A_π data, corrected for radiative effects, are plotted versus c.m. scattering angle. The dashed curve corresponds to no charge symmetry breaking and is incompatible with our data. The solid line corresponds to $C_W=4.35$ MeV and the dotted-dashed line to $C_W=3.6$ MeV (see text). All curves include the neutron proton mass difference.

The inclusion of a charge symmetry breaking term C_W is required for agreement between data and calculations.

Theoretical curves through the data are shown corresponding to $C_W=4.35$ MeV (solid line) and 3.6 MeV (dotted-dashed line). The solid curve was obtained by ignoring the bump in the data near 100° , which cannot be reproduced by present πd theories, and determining that value of C_W which best fits the data below 90° and above 110° . The value of C_W obtained by a χ^2 fit is 4.35 ± 0.50 MeV, and is not a legitimate representation of all our data but it prevents undue weighting by an angular region in which the differential cross section is a minimum (~ 1 mb/sr). The principal effect of varying the C_W parameter is to shift the curve up or down without a significant change in shape. Consequently it is not possible, with only one free parameter describing charge symmetry breaking in terms of mass (and width) differences among the components of the delta, to describe structure which deviates from this curve. Any such deviation, if it is statistically significant, must reflect some additional charge symmetry violating feature of the $\pi^\pm d$ interactions, perhaps occurring in a higher partial wave. We feel that $C_W=4.35 \pm 0.50$ MeV best describes the overall envelope of data measured in this study.

A possibly more legitimate estimate of C_W may be obtained by finding that value of C_W which minimizes the χ^2 of all the measured data including the bump near 100° . This somewhat overestimates the data at forward and back angles, while underestimating the region near 100° , as is shown in the dotted-dashed line in Fig. 6. A value of 3.6 ± 0.6 MeV is obtained for the charge symmetry breaking parameter C_W in this manner, and the χ^2 of the fit is naturally larger.

The values of χ^2/N obtained in each case are 0.4 and 0.8, respectively. The fact that the χ^2/N values are less than 1 reflects the errors in the theoretical $\pi^\pm p$ cross sections. These were taken from the SCATPI (Ref. 63) computer program and reflect an absolute error at each angle, whereas the relative error between adjacent angles is considerably less.

Two new theoretical corrections have been presented here, corresponding to charge symmetry breaking due to mass differences among the components of the delta and to the effect of the Coulomb interaction on the strong πd phases, evaluated in terms of a difference in effective nuclear interaction energies. These two effects are approximately equal in magnitude and opposite in

sign, bringing the final calculation close to the result presented in our initial Letter.¹ The sign of the term involving the C_W parameter [Eq. (4.22) or (4.23)] changes as the energy is increased above the 3-3 resonance. Thus our experimental data at 256 MeV, presently being analyzed, will provide a check on the parametrization of the charge symmetry breaking part of this interaction in terms of C_W .

V. CONCLUSIONS

Our measurements of differential cross sections for $\pi^\pm d$ elastic scattering have tested charge symmetry in the region below the 3-3 resonance. Care was taken in our experimental procedures to ensure an accurate measurement of the difference between $\pi^+ d$ and $\pi^- d$ differential cross sections. We have also obtained the first accurate $\pi^- d$ differential cross sections in this energy region.

The experimental analysis included corrections for radiative effects. Absolute normalizations were based on the charge dependent $\pi^\pm d$ phase shift analysis of Carter, Bugg, and Carter.⁶⁴ We have also estimated systematic differences which could arise from the use of the VPI charge dependent $\pi^\pm d$ phase shift analysis.⁶⁸

Theoretical analysis was based on three-body calculations of the πd interaction. Within this framework we have made corrections for Coulomb scattering, Coulomb-nuclear interference, and Coulomb effects on the strong phase shifts.

Our data show a definite violation of charge symmetry. Even the extreme values of our data permitted by the error analysis are not compatible with charge symmetry. The use of the VPI $\pi^\pm p$ phases⁶⁸ instead of those of Carter, Bugg, and Carter⁶⁴ would make the charge symmetry violation even larger, increasing the value of C_W by 1.4 MeV.

The observed violation of charge symmetry has been parametrized in terms of mass and width differences among the components of the Δ isobar. The major sensitivity is to the mass difference parameter C_W . This parametrization gives a good description of the data except in the region of minimum cross section near 100° , with a best fit value of $C_W=4.35 \pm 0.50$ MeV. We consider this to be the best estimate of C_W within the context of the present theory.

The bump seen in the data near 100° is statistically significant but not describable in terms of mass and width parameters of the Δ isobar. The rapid angular change suggests the presence of higher par-

tial waves. Taking a best fitted mean value which slightly underestimates the data in the 100° region and slightly overestimates it everywhere else would lower the value of C_W by 0.75 MeV. A better understanding of any such effects, which fall outside of present theoretical considerations, can best be obtained by repeating this experiment at 180 MeV. At this energy (the center of the 3-3 resonance) the coefficient of the C_W parameter [Eq. (4.22)] is zero and isolation of other effects becomes possible.

The value of C_W obtained by Pedroni *et al.*² in their analysis of the energy dependence of the $\pi^\pm d$ total cross section data was 4.6 ± 0.2 MeV, where their quoted error is purely statistical. Their measurements were absolute and consequently independent of ambiguities in $\pi^\pm p$ phase shift analyses. Our data and theirs are in good agreement. Our data are also in agreement with the MIT bag model calculations of Bickerstaff and Thomas⁷⁹ who obtain $C_W = 4.47$ MeV.

Our results may be compared to the unsuccessful searches⁸⁰ for charge symmetry violation, at higher total energy, in the π^0 producing reactions $d + d \rightarrow {}^4\text{He} + \pi^0$ and $n + p \rightarrow d + \pi^0$. (See, however, Ref. 2 regarding hindrance factors in these cross sections.)

An additional check on the magnitude of the charge symmetry breaking is underway at 256 MeV where the sign of the coefficient of the C_W parameter is opposite that at 143 MeV. At even higher energies the magnitude of the effect should decrease. Another measurement in the energy region near 100 MeV would help greatly in providing a consistent description of charge symmetry breaking effects parametrizable in terms of mass differences among the components of the delta isobar. Finally, charge symmetry violating effects which are largely independent of Δ mass differences can best be examined by a careful comparison of $\pi^\pm d$ differential cross sections at 180 MeV.

ACKNOWLEDGMENTS

We would like to thank the staff of LAMPF for extensive experimental and computational support. The assistance of C. Morris, D. A. Lind, and N. S. P. King during data collection was particularly appreciated. We are grateful to M. Stanton for help in experimental data analysis and we would like to thank E. Siciliano and G. A. Miller for discussions on theoretical matters and B. Blankleider for pro-

viding πd phases from Ref. 34. This work was supported in part by the U. S. Department of Energy.

APPENDIX A

The absolute values of the $\pi^\pm d$ cross sections listed in Table II are directly dependent on the set of $\pi^\pm p$ phases used. We have used the charge dependent $\pi^\pm p$ phases of Carter, Bugg, and Carter.⁶⁴ In order to evaluate the effect of other sets of $\pi^\pm p$ phases, we have calculated and plotted in Fig. 7 the ratio of differential cross sections calculated from

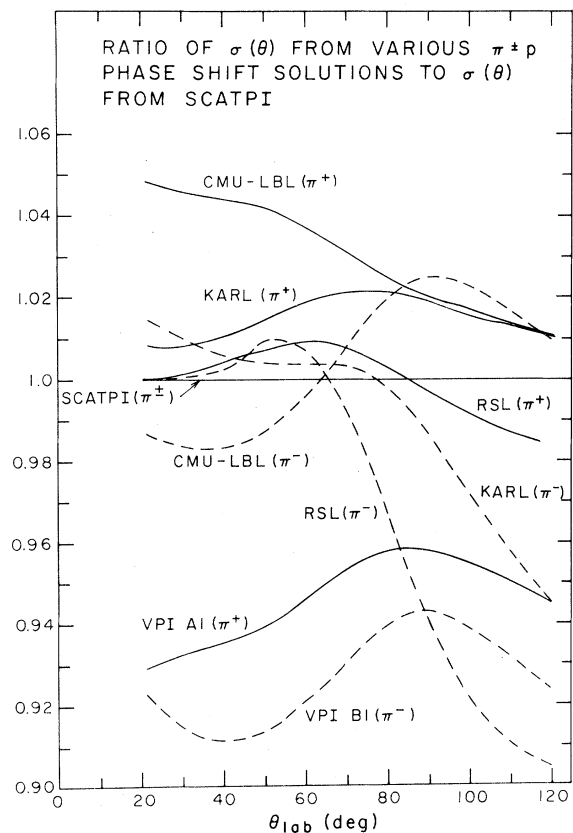


FIG. 7. Comparison of $\pi^\pm p$ cross sections calculated by various phase shift programs. All ratios are calculated relative to the SCATPI code which is indicated by the straight line at 1.0 for both $\pi^\pm p$ and is based on the Carter, Bugg, and Carter phase shifts (Ref. 64). Relative values are shown for Karlsruhe (Ref. 67), VPI (Ref. 68), CMU-LBL (Ref. 65), and Rowe-Salomon-Landau (Ref. 66) phase shifts. The π^+ comparisons are shown as solid lines while π^- comparisons are shown as dashed lines. Absolute magnitudes of the predicted cross sections are seen to vary from +5 to -9% over the angular region of interest. The SCATPI and VPI A1 (for π^+) and VPI B1 (for π^-) calculations are the only ones which do not explicitly assume charge independence.

these phase shifts and cross sections calculated from Karlsruhe,⁶⁷ CMU-LBL,⁶⁵ VPI,⁶⁸ and Rowe, Salomon, and Landau⁶⁶ phase shifts. The differences range from -9% to $+5\%$, and the uncertainty in the absolute values of the πd differential cross sections is linearly dependent on this difference. The systematic uncertainty in the asymmetry data depends only on the relative difference between π^+p and π^-p cross sections (see text). Of these other sets of $\pi^\pm p$ phase shifts, only the VPI phase shifts (VPI A 1 for π^+p , VPI B 1 for π^-p) do not explicitly assume isospin invariance and consequently this is the only other set of $\pi^\pm p$ phases which could be used in our analysis.

APPENDIX B

The matrix element $\tau_l(E)$ for πd elastic scattering has the form

$$\begin{aligned} \tau_l(E) &= e^{i\delta_l(E)} \sin\delta_l(E) \\ &= \frac{\Gamma_{el}^l}{2(E_R^l - E) - i\Gamma^l} \end{aligned} \quad (\text{B1})$$

if we assume a Breit-Wigner shape, where Γ and Γ_{el} are the total and elastic widths, respectively, E_R is the resonance energy, and l refers to the l th partial wave. The width Γ is also energy dependent:

$$\Gamma(k) = \Gamma_0 \frac{k^3}{k_0^3} \frac{1+k_0^2 a^2}{1+k^2 a^2}. \quad (\text{B2})$$

Using Taylor's theorem to expand in E , we obtain

$$\begin{aligned} \Delta\tau_l(E) &= \left[\frac{2\delta E_l}{\Gamma_{el}^l} \tau_l(E) + \frac{(3+a^2 k^2)}{(1+a^2 k^2)} \frac{\omega_k \delta E_l}{k^2} \right. \\ &\quad \left. \times \left\{ 1 + i \frac{\Gamma^l}{\Gamma_{el}^l} \tau(E) \right\} \right] \tau(E), \end{aligned} \quad (\text{B3})$$

where

$$\omega_k = (k^2 + m_\pi^2)^{1/2},$$

k is the c.m. momentum, $a = 1.15$ fm, and δE_l is the small shift in the effective interaction energy in channel l . This Coulomb energy shift is evaluated at a πN c.m. energy of 115 MeV to correspond to πd scattering at 143 MeV in the laboratory.

The scattering amplitude describing a resonance in the complex s plane has the form³

$$f_{0i} = \frac{W_{0i} \Gamma_{ei}}{(W_{0i}^2 - W^2) - iW_{0i} \Gamma_{ii}}, \quad (\text{B4})$$

where W is the total energy in the πN system, W_{0i} is the mass of the pion-nucleon i th Δ isobar, and Γ_{ii} and Γ_{ei} are their total and elastic widths. For the P_{33} resonance we can replace the elastic width by the total width by noting that

$$\begin{aligned} \Gamma_{e++,-} &= \Gamma_{t++,-}, \\ \Gamma_{e+,-,+} &= \frac{1}{3} \Gamma_{t+,-,+}, \end{aligned} \quad (\text{B5})$$

and considering the amplitude difference

$$f_{0--} - f_{0++} + (f_{0-+} - f_{0+-})/3.$$

Expanding (B4) in terms of the average delta mass W_0 and a mean total width Γ_t we obtain

$$\begin{aligned} f_{0i} &= f_0 \left[1 + \frac{\delta\Gamma_{ii}}{\Gamma_t} + \frac{\delta W_{0i}}{W_0} \right. \\ &\quad \left. - f_0 \left\{ 2 \frac{\delta W_{0i}}{\Gamma_t} - i \frac{\delta W_{0i}}{W_0} - i \frac{\delta\Gamma_{ii}}{\Gamma_t} \right\} \right], \end{aligned} \quad (\text{B6})$$

where

$$f_0 = W_0 \Gamma_t / (W_0^2 - W^2 - iW_0 \Gamma_t).$$

Neglecting terms in $\delta W_{0i}/W_0$ since W_0 is an order of magnitude larger than Γ_t , we obtain

$$\begin{aligned} f_{0--} - f_{0++} + \frac{1}{3}(f_{0-+} - f_{0+-}) &= \frac{f_0}{\Gamma_t} [\delta\Gamma_{--} - \delta\Gamma_{++} + \frac{1}{3}(\delta\Gamma_{-+} - \delta\Gamma_{+-}) \\ &\quad - f_0 \{ 2(\delta W_{--} - \delta W_{++} + \frac{1}{3}(\delta W_{-+} - \delta W_{+-})) \\ &\quad - i(\delta\Gamma_{--} - \delta\Gamma_{++} + \frac{1}{3}(\delta\Gamma_{-+} - \delta\Gamma_{+-})) \}]. \end{aligned} \quad (\text{B7})$$

Defining after Pedroni *et al.*²

$$\begin{aligned} C_W &= W_{--} - W_{++} + \frac{1}{3}(W_{-+} - W_{+-}) \\ &= \delta W_{--} - \delta W_{++} + \frac{1}{3}(\delta W_{-+} - \delta W_{+-}) \end{aligned} \quad (\text{B8})$$

and

$$\begin{aligned} \tilde{C}_\Gamma &= \Gamma_{t--} - \Gamma_{t++} + \frac{1}{3}(\Gamma_{t-+} - \Gamma_{t+-}) \\ &= \delta \Gamma_{t--} - \delta \Gamma_{t++} + \frac{1}{3}(\delta \Gamma_{t-+} - \delta \Gamma_{t+-}), \end{aligned} \quad (\text{B9})$$

we obtain

$$\begin{aligned} f_{0--} - f_{0++} + \frac{1}{3}(f_{0-+} - f_{0+-}) \\ = \epsilon_{--} - \epsilon_{++} + \frac{1}{3}[\epsilon_{-+} - \epsilon_{+-}] \\ = \frac{f_0}{\Gamma_t} [\tilde{C}_\Gamma - f_0(2C_W - i\tilde{C}_\Gamma)]. \end{aligned} \quad (\text{B10})$$

*Present address: Division TH, CERN, 1211 Geneva 23, Switzerland.

- ¹T. G. Masterson *et al.*, Phys. Rev. Lett. **47**, 220 (1981).
²E. Pedroni *et al.*, Nucl. Phys. **A300**, 321 (1978).
³F. Myhrer and H. Pilkuhn, Z. Phys. A **276**, 29 (1976).
⁴L. D. Faddeev, Zh. Eksp. Teor. Fiz. **39**, 1459 (1960) [Sov. Phys.—JETP **12**, 1014 (1961)].
⁵P. J. Bussey *et al.*, Nucl. Phys. **B58**, 363 (1973).
⁶E. G. Pewitt, T. H. Fields, G. B. Yodh, J. G. Fetkovich, and M. Derrick, Phys. Rev. **131**, 1826 (1963).
⁷K. Gabathuler *et al.*, Nucl. Phys. **A350**, 253 (1980).
⁸N. Giraud, C. Fayard, and G. H. Lamot, Phys. Rev. C **21**, 1959 (1980).
⁹A. W. Thomas, Nucl. Phys. **A258**, 417 (1976).
¹⁰A. S. Rinat and A. W. Thomas, Nucl. Phys. **A282**, 365 (1977).
¹¹A. S. Rinat, Nucl. Phys. **A287**, 399 (1977).
¹²A. S. Rinat, E. Hammel, Y. Starkand, and A. W. Thomas, Nucl. Phys. **A329**, 285 (1979).
¹³F. Myhrer and D. S. Koltun, Phys. Lett. **46B**, 322 (1973); Nucl. Phys. **B86**, 441 (1975).
¹⁴I. R. Afnan and A. W. Thomas, in *Proceedings of the International Conference on Few Particle Problems in Nuclear Interaction, Los Angeles, 1972*, edited by I. Slaus *et al.* (North-Holland, Amsterdam, 1973), p. 861.
¹⁵C. Carlson, Phys. Rev. C **2**, 1224 (1970); M. McMillan and R. H. Landau, TRIUMF Report, TRI-74-1, 1974.
¹⁶M. M. Hoenig and A. S. Rinat, Phys. Rev. C **10**, 2102 (1974).
¹⁷T. Mizutani and D. Koltun, Ann. Phys. (N.Y.) **109**, 1 (1977).
¹⁸A. W. Thomas, *Proceedings of the International Conference on Few Body Problems in Nuclear and Particle Physics*, edited by R. J. Slobodrian, B. Cujec, and K. Ramavataram (Les Presses de l'Université Laval, Quebec, 1975), p. 287.
¹⁹N. M. Petrov and V. V. Peresypkin, Phys. Lett. **44B**, 321 (1973).
²⁰A. W. Thomas and I. R. Afnan, Phys. Lett. **45B**, 437 (1973).
²¹F. Myhrer, Nucl. Phys. **B80**, 491 (1974).
²²F. Myhrer and D. S. Koltun, Nucl. Phys. **B86**, 441

(1975).

- ²³F. Myhrer, Nucl. Phys. **A241**, 524 (1975).
²⁴T. I. Kopaleishvili, A. I. Machavariani, and G. A. Emelyanenko, Joint Institute for Nuclear Research Report JINR, E4-9951, 1976.
²⁵R. M. Woloshyn, E. J. Moniz, and R. Aaron, Phys. Rev. C **13**, 286 (1976).
²⁶N. Giraud, Y. Avishai, C. Fayard, and G. H. Lamot, Phys. Rev. C **19**, 465 (1979).
²⁷A. S. Rinat, Y. Starkand, E. Hammel, and A. W. Thomas, Phys. Lett. **80B**, 166 (1979).
²⁸C. Fayard, G. H. Lamot, and T. Mizutani, Phys. Rev. Lett. **45**, 524 (1980).
²⁹A. W. Thomas and A. S. Rinat, Phys. Rev. C **20**, 216 (1979).
³⁰B. Blankleider and I. R. Afnan, Phys. Rev. C **22**, 1638 (1980).
³¹Y. Avishai and T. Mizutani, Nucl. Phys. **A326**, 352 (1979); **A338**, 377 (1980); **A352**, 399 (1981); University of Lyon report, 1980.
³²I. R. Afnan and A. W. Thomas, Phys. Rev. C **10**, 109 (1974).
³³A. W. Thomas and R. H. Landau, Phys. Rep. **58**, 121 (1980).
³⁴B. Blankleider and I. R. Afnan, Phys. Rev. C **24**, 1572 (1981); Phys. Lett. **93B**, 367 (1980).
³⁵C. Fayard, G. H. Lamot, and T. Mizutani, Phys. Rev. Lett. **45**, 524 (1980); University of Lyon report, 1981 (unpublished).
³⁶J. Bolger *et al.*, Phys. Rev. Lett. **46**, 167 (1981).
³⁷R. J. Holt *et al.*, Phys. Rev. Lett. **43**, 1229 (1979); **47**, 472 (1981).
³⁸W. Grüebler, private communication; J. Ulbricht *et al.*, Phys. Rev. Lett. **48**, 311 (1982).
³⁹K. Kubodera, M. P. Locher, F. Myhrer, and A. W. Thomas, J. Phys. G **6**, 171 (1980).
⁴⁰J. Arvieux and A. S. Rinat, Nucl. Phys. **A350**, 205 (1980).
⁴¹E. M. Henley and G. A. Miller, in *Mesons in Nuclei*, edited by M. Rho and D. Wilkinson (North-Holland, Amsterdam, 1979), Vol. I, p. 405.
⁴²G. Breit, K. A. Friedman, J. M. Holt, and R. E. Seamon, Phys. Rev. **170**, 1424 (1968); P. U. Sauer,

- Phys. Rev. Lett. 32, 626 (1974); A. W. Thomas and I. R. Afnan, Phys. Lett. 55B, 425 (1975).
- ⁴³P. Langacker and D. A. Sparrow, Phys. Rev. Lett. 43, 1559 (1979).
- ⁴⁴A. W. Thomas, P. Bickerstaff, and A. Gersten, Phys. Rev. D 24, 2539 (1981).
- ⁴⁵Proceedings of the Charge Symmetry Breaking Workshop, Vancouver, 1981, edited by N. E. Davison *et al.*, Report TRI-81-3, 1981 (unpublished).
- ⁴⁶S. Fiarman and S. S. Hanna, Nucl. Phys. A251, 1 (1975).
- ⁴⁷J. A. Tjon, Nucl. Phys. A353, 47c (1981).
- ⁴⁸K. Okamoto, Phys. Lett. 19, 676 (1966).
- ⁴⁹W. Grüebler, Nucl. Phys. A353, 31c (1981).
- ⁵⁰C. L. Hollas *et al.*, Phys. Rev. C 24, 1561 (1981).
- ⁵¹K. C. Rogers and L. M. Lederman, Phys. Rev. 105, 247 (1957).
- ⁵²J. H. Norem, Nucl. Phys. B33, 512 (1971).
- ⁵³K. Gabathuler *et al.*, Nucl. Phys. B55, 397 (1973).
- ⁵⁴D. Axen *et al.*, Nucl. Phys. A256, 387 (1976).
- ⁵⁵R. H. Cole *et al.*, Phys. Rev. C 17, 681 (1978).
- ⁵⁶R. C. Minehart *et al.*, Phys. Rev. Lett. 46, 1185 (1981).
- ⁵⁷A. Stanovic *et al.*, Phys. Lett. 94B, 323 (1980).
- ⁵⁸L. S. Dulkova, I. B. Sokolova, and M. G. Shafranova, Zh. Eksp. Teor. Fiz. 35, 313 (1958) [Sov. Phys.—JETP 8, 217 (1959)].
- ⁵⁹B. Balestri *et al.*, Proceedings of 9th International Conference on High Energy Physics and Nuclear Structure, Versailles, 1981 (unpublished), p. 298.
- ⁶⁰W. Plessas, L. Streit, and H. Zingl, Acta Phys. Austriaca 40, 272 (1974).
- ⁶¹C. Richard-Serre *et al.*, Nucl. Phys. B20, 413 (1970).
- ⁶²H. A. Thiesen *et al.*, Los Alamos Informal Report LA-6663-MS, 1977 (unpublished); R. L. Boudrie *et al.*, IEEE Trans. Nucl. Sci. NS26, 4588 (1979); J. F. Amann *et al.*, *ibid.* NS26, 4389 (1979); L.G. Atencio *et al.*, Nucl. Instrum. Methods 187, 381 (1981).
- ⁶³SCATPI, a subroutine for calculating πN cross sections and polarizations for incident pion energies between 90 and 300 MeV, J. B. Walter and G. A. Rebka, Los Alamos Report UC34A, 1979 (unpublished).
- ⁶⁴J. R. Carter, D. V. Bugg, and A. A. Carter, Nucl. Phys. B58, 378 (1973).
- ⁶⁵D. J. Hendon *et al.*, University of California Radiation Laboratory Report No. UCRL-20030, 1970 (unpublished); L. D. Roper, private communication.
- ⁶⁶G. Rowe, M. Salomon, and R. Landau, Phys. Rev. C 18, 584 (1978).
- ⁶⁷G. Höhler, F. Kaiser, R. Koch, and E. Pietarinen, *Handbook of Pion-Nucleon Scattering* (Fachinformationszentrum Karlsruhe, Karlsruhe, 1979).
- ⁶⁸L. D. Roper and R. A. Arndt, private communication.
- ⁶⁹E. Borie, Phys. Lett. 68B, 433 (1977).
- ⁷⁰L. P. Kok, in *Proceedings of the Ninth International Conference on the Few Body Problem*, edited by F. S. Levin (North-Holland, Amsterdam, 1981); Nucl. Phys. A353, 171c (1981).
- ⁷¹C. Chandler, Nucl. Phys. A353, 129c (1981).
- ⁷²E. O. Alt, W. Sandhas, and H. Ziegelmann, Phys. Rev. C 17, 1981 (1978).
- ⁷³S. Merkuriev, Freie Universität Berlin/Hoch energie Physik Report 2/81, 1980.
- ⁷⁴L. P. Kok and H. van Haeringen, Phys. Rev. C 21, 512 (1980).
- ⁷⁵J.-F. Germond and C. Wilkin, Ann. Phys. (N.Y.) 121, 285 (1979).
- ⁷⁶D. S. Koltun, in *Advances in Nuclear Physics*, edited by E. V. Baranger and E. Vogt (Plenum, New York, 1969), Vol. 3, p. 71.
- ⁷⁷H. A. Bethe and F. de Hoffman, *Mesons and Fields* (Row and Peterson, Evanston, 1955), Vol. II, p. 63.
- ⁷⁸H. R. Rubinstein, F. Scheck, and R. H. Socolow, Phys. Rev. 154, 1608 (1967); H. R. Rubinstein, Phys. Rev. Lett. 17, 41 (1966).
- ⁷⁹R. P. Bickerstaff and A. W. Thomas, Phys. Rev. D 25, 1869 (1982).
- ⁸⁰J. Banaigs *et al.*, Phys. Lett. 53B, 390 (1974).